INVESTIGATION OF SPATIALLY NON-UNIFORM DEFECT PASSIVATION IN EFG Si BY SCANNING PHOTOLUMINESCENCE TECHNIQUE

Kenta Nakayashiki and Ajeet Rohatgi
School of Electrical and Computer Engineering
Georgia Institute of Technology, Atlanta, GA 30332

Igor Tarasov and Sergei Ostapenko
Nanomaterials and Nanomanufacturing Research Center
University of South Florida, Tampa, FL 33620

Lynn Gedvilas and Brian Keyes
National Renewable Energy Laboratory, Golden, CO 80401

Bala R. Bathey and Juris P. Kalejs
RWE Schott Solar, Inc., Billerica, MA 01821

ABSTRACT

This paper shows that both hydrogenation of defects from SiN_x coating and thermally-induced dehydrogenation of defects are rapid and occur simultaneously in EFG Si during cell processing. Room-temperature scanning photoluminescence mappings, before and after the SiN_x-induced hydrogenation, revealed that hydrogenation of defective regions is effective and pronounced, with more than an order of magnitude increase in lifetime, compared to the rest of the bulk. In addition, FTIR measurements showed the concentration of bonded hydrogen in the SiN_x film decreases with the increase in annealing temperature and time. However, the rate of release of hydrogen from the SiN_x film decreases sharply after the first few seconds. Based on this understanding, a process was developed for a co-firing of SiN_x film and screen-printed Al and Ag in RTP unit, which produced 4 cm^2 EFG Si cell with highest efficiency of 16.1%.

INRDODUCTION

Edge-defined film-fed grown (EFG) ribbon Si is one of the promising candidates to achieve low-cost and high-efficiency solar cells. Due to the direct contact between the Si melt and the shaping die and high thermal stresses during the material growth, EFG Si has high density of defects such as dislocations and grain boundaries, along with relatively high concentrations of transition metal impurities that act as recombination centers [1]. These defects lead to very low as-grown bulk lifetime in the range of 1-3 μs. Therefore, it is necessary to enhance carrier lifetime during the solar cell fabrication process in order to achieve high-efficiency cells on low-cost and defective EFG Si. Impurity gettering during P diffusion, Al-doped back surface field formation, and hydrogenation from the amorphous SiN_x anti-reflection (AR) layer during contact firing are frequently used in industry with varying degree of success. In addition, there is limited quantitative understanding of the degree and spatial uniformity of defect hydrogenation. Therefore, the scanning room-temperature photoluminescence (PL) spectroscopy is used in this paper to study the degree and rate of hydrogenation and dehydrogenation of highly as well as less defective regions in the EFG Si. Fourier Transform Infrared (FTIR) measurements are also performed on the SiN_x films deposited on float zone (FZ) Si substrates to study the impact of firing cycle on the rate of release of bonded hydrogen from the SiN_x film. PL measurements after the SiN_x-induced hydrogenation and subsequent dehydrogenation after SiN_x removal and anneal are used to assess the rate of dehydrogenation of defects. Improved understanding of the competition between hydrogenation and dehydrogenation of defects is used to establish the optimum firing cycle for effective defect passivation and achieve high-efficiency screen-printed EFG Si solar cells.

EXPERIMENT

Scanning photoluminescence mappings in EFG Si

In this study, B-doped 300 μm thick EFG Si wafers with resisitivty of 3-4 Ω·cm from RWE Schott Solar were used. An 800 nm pulse AlGaAs laser diode with 140 mW peak power was used for the PL excitation. Details of PL mapping set-up and procedure have been published in [2]. Along with the finding that the PL spectrum of mc-Si materials, like EFG Si, at room-temperature contains two luminescence bands. First band (I_{BB}) shows a spectral maximum at 1.08 eV and corresponds to direct band-to-band recombination of electron-hole pairs in Si [3]. The second "defect" band at ~0.8 eV (I_{Def}) is observed only in the selected regions and corresponds to deep luminescent defects located around the dislocations [4]. This defect band is a fingerprint for the highly defective low lifetime regions in EFG Si wafers and is associated with the dislocations decorated with impurity precipitates [2]. PL maps with reasonable spatial resolution can be used to deduce the (a) distribution of the effective minority carrier

0-7803-8707-4/05/$20.00 ©2005 IEEE.

lifetime (τ_{eff}) [5], (b) lifetime variation after a solar cell processing, and (c) maps of the defect centers responsible for 0.8 eV PL band. The τ_{eff} is composed of radiative, non-radiative, and surface recombinations and is generally dominated by non-radiative recombination in Si. In a simple case, neglecting diffusion of the photogenerated minority carriers, the I_{BB} and I_{Def} can be expressed as follows [2]:

$$I_{BB} = C_1 \times G \times \tau_{eff} / \tau_{rad} \quad (1)$$

$$I_{Def} = C_2 \times G \times \tau_{eff} / \tau_{SRH} \quad (2)$$

$$\tau_{SRH} = (N_{Def} v_{th} \sigma_n) \quad (3)$$

where G is the electron-hole pair photo-generation rate, τ_{rad} is the radiative band-to-band recombination lifetime, τ_{SRH} is the radiative component of Shockley–Read–Hall lifetime, N_{Def} is the radiative defect concentration, v_{th} and σ_n are the electron thermal velocity and capture cross section, C_1 and C_2 are temperature dependent Si constants. A new parameter, $R = I_{Def}/I_{BB}$, is introduced to measure the point-by-point ratio of two PL intensities. From Eqs. (1) to (3), it is clear that

$$R = I_{Def} / I_{BB} = const \times N_{Def}. \quad (4)$$

Thus R-parameter map can give the spatial distribution of radiative PL defect concentration. Notice that the R-parameter is independent of other recombination defects in the bulk and at the surface, which influence the τ_{eff}. Scanning PL measurements were performed on the same sample 1) before hydrogenation, 2) after hydrogenation and SiN_x removal, and 3) after dehydrogenation anneal.

Detection of N-H and Si-H bonds in SiN_x film by FTIR measurements

FTIR measurements were performed on low-frequency PECVD SiN_x films deposited on high resistivity (500-1000 Ω·cm) n-type FZ Si wafers to determine the change in concentration of N-H and Si-H bonds in the deposited SiN_x film as a function of annealing temperature and time. Prior to the SiN_x deposition, FZ Si wafers were etched and cleaned in chemical solutions. SiN_x film with a refractive index of 2.0 was deposited on both sides of the substrate.

RESULTS AND DISCUSSIONS

Improved understanding of hydrogenation and dehydrogenation in EFG Si

Table I shows the average values of I_{BB}, I_{Def}, and R-paraemter on the same EFG Si sample after 1) initial PL measurement prior to SiN_x deposition, 2) SiN_x deposition followed by 750°C/1 s hydrogenation in an RTP unit with Al on the back, 3) SiN_x and Al removal followed by 600°C/1 s and 700°C/1 s dehydrogenation anneals. The data analysis revealed that area-averaged I_{BB}, which is proportional to the effective carrier lifetime, increased from 29 to 126 (arb.un.) after the 750°C/1 s hydrogenation. EFG Si wafers were then reannealed after SiN_x and Al removal to study the dehydrogenation of defects. In the absence of SiN_x film, the I_{BB} decreased from 126 to 113 and 42 after the subsequent 600°C/1 s and 700°C/1 s dehydrogenation anneals, respectively. Substantial reduction in I_{BB} supports rapid dissociation of hydrogen from defects at 700°C in the absence of hydrogen supply. Fig. 1 shows the PL mappings of the EFG Si sample described above. Fig. 2 shows the results of a line-scan through the above sample at a specific location to assess spatial variation in the reduction of effective lifetime (I_{BB}(dehydrogenated)/I_{BB}(hydrogenated)) after 700°C/1 s dehydrogenation. Fig. 2 also shows the radiative defect concentration or R-parameter after 750°C/1 s hydrogenation and subsequent 700°C/1 s dehydrogenation. The R-parameter is high or impurity-decorated dislocations are the primary carrier recombination centers. In addition, the R-parameter is appreciable in the highly defective regions even after the 750°C/1 s hydrogenation, indicating that all the defects are not fully passivated in EFG Si even when the hydrogenation increased the average bulk lifetime from 3 μs to ~100 μs. Average lifetime was measured quasi steady-state photoconductance technique at an injection level of 1.0×10^{15} cm^{-3} [6] before and after hydrogenation. Lifetime was measured and averaged over thirty-two different locations in several wafers. Fig. 2 shows that 700°C/1 s dehydrogenation leads to largest reduction in I_{BB} or effective lifetime in the highly defective regions. Table I and Fig. 2 demonstrate that the R-parameter increases dramatically in the defective regions after the 700°C/1 s dehydrogenation (R(dehydrogenated) > R(hydrogenated)), clearly indicating that significant defect dehydrogenation takes place in the areas with high defect density. This is further supported by the increase in average R-parameter, which is proportional to the radiative defect concentration, from 0.0111 to 0.0237 after the 700°C/1 s dehydrogenation. Fig. 2 also shows that the reduction in the effective lifetime (I_{BB}(dehydrogenated) / I_{BB}(hydrogenated)), which is caused by the increase in non-radiative recombination centers, seems to occur concurrently with increase in R-parameter or radiative recombination centers.

Table 1. Average values of PL intensities.

	I_{BB}	I_{Def}	R-parameter
(1) Initial	28.81	n.a.*	n.a.*
(2) 750°C/1 s hydrogenation	126.33	0.708	0.0111
(3) 600°C/1 s dehydrogenation	112.47	0.613	0.0127
(3) 700°C/1 s dehydrogenation	42.80	0.339	0.0237

* below sensitivity limit

FTIR measurements to assess the bonded hydrogen concentration in SiN_x film as a function of annealing

FTIR measurements were performed as a function of annealing time and temperature to track the change in the bonded hydrogen content of SiN_x film in an attempt to understand the rate of hydrogen supply. FTIR measurements on SiN_x film deposited on FZ Si substrate showed two distinct peaks, at 3340 cm^{-1} and 2180 cm^{-1}, corresponding to N-H and Si-H bonds, respectively [7,8]. The dissociation of bonded hydrogen in the SiN_x film is generally considered as a source for hydrogen passivation of defects [9]. The absolute concentrations of N-H and Si-H bonds were determined from the area of their respective peaks, using the correlation coefficients in [10], after converting transmittance to absorbance. Fig. 3 shows the concentration of total bonded hydrogen in the SiN_x film after various heat treatments in an RTP unit. A rapid decrease in bonded hydrogen content was observed when SiN_x film was annealed at high temperature (>750°C). Equally important is the fact that this decrease is rapid initially (≤1 s) and then slows down. This suggests that the SiN_x film provides a limited source of hydrogen and its supply decreases rapidly as the annealing time exceeds ~1 s. Since the dehydrogenation continues at a steady pace, shorter firing time provides more effective defect passivation.

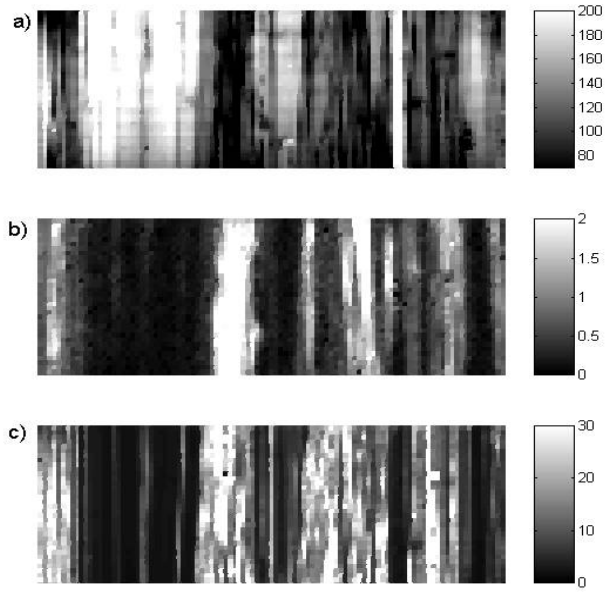

Fig. 1: PL maps of (a) band-to-band PL (I_{BB}), (b) defect band PL (I_{Def}), and (c) point by point ratio of I_{BB}(hydrogenated)/I_{BB}(initial) representing the increase in lifetime. The mapping size is 50 ×22 mm^2, step = 0.5 mm.

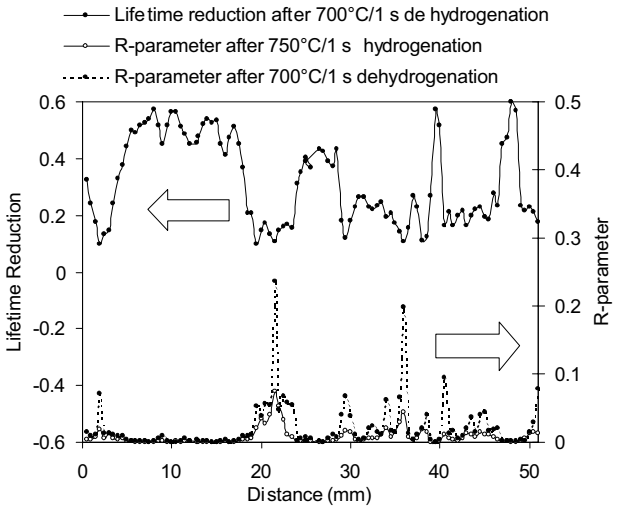

Fig. 2: Line-scan through a PL map to quantify loss of carrier lifetime (I_{BB}(hydrogenated)/I_{BB}(dehydrogenated)) and R-parameters (I_{Def}/I_{BB}) changes after hydrogenation and 700°C/1 s dehydrogenation.

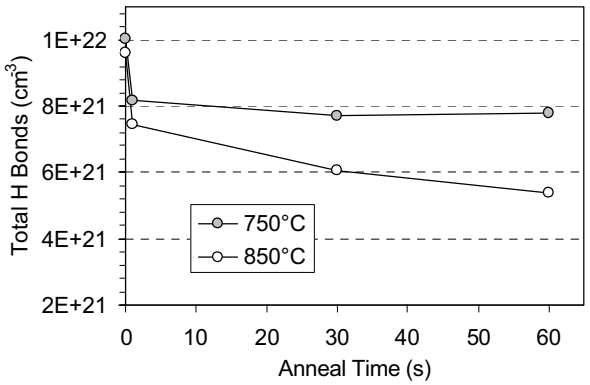

Fig. 3: Decrease in concentration of hydrogen bonds (N-H and Si-H) in SiN_x film as a function of annealing time.

Solar cell fabrication

Based on the above analysis of hydrogen passivation and dissociation of defects, a rapid co-firing of screen-printed Al and Ag was developed to enhance the SiN_x-induced hydrogenation of defects. After the initial cleaning, EFG Si wafers were P diffused to form n^+ emitter layer with a sheet resistance of 40-50 Ω/sq. A SiN_x AR coating with a thickness of 750 Å and a refractive index of 2.0 was deposited in a low-frequency PECVD reactor. Al and Ag pastes were screen printed on the back and front, respectively. Finally, each cell was isolated by dicing saw. Nine 4 cm^2 cells were fabricated on each wafer.

Table II shows the average solar cell parameters for the 34 cells along with the best screen-printed EFG Si cell parameters. Average efficiency was 15.2% with highest efficiency of 16.1%. These results were confirmed by NREL.

Table II: Solar cell parameters

	V_{OC} (mV)	J_{SC} (mA/cm^2)	FF	Eff. (%)	# of cells
Average	596	33.21	0.766	15.2	34
Best	613	34.02	0.772	16.1	

CONCLUSION

Room-temperature PL measurements showed that defective or low lifetime regions are strongly passivated during the hydrogenation step. In highly defective regions, lifetime increased by as much as a factor of 50 while less defective regions showed an increase of less than a factor of three. It was found that dehydrogenation is also rapid in these defective regions. FTIR measurements on SiN_x deposited FZ Si wafer revealed that the bonded hydrogen concentration in SiN_x film decreases as a function of annealing time and temperature, and the rate of release slows down with time at a given temperature. This indicates that the supply of hydrogen from SiN_x film is limited. Since the thermally-induced dehydrogenation of defects is expected to continue at the same rate at a given temperature, effectiveness of hydrogenation should decrease for prolonged firing.

Rapid hydrogenation and dehydrogenation of defects, which happen simultaneously during contact firing of cells, gave rise to an optimum hydrogenation cycle of 750°C/1 s for EFG Si. This cycle produced 4 cm^2 screen-printed EFG Si solar cells with efficiency of ≥16%.

ACKNOWLEDGMENT

This work was supported in part by NREL (Contract Nos. ACQ-9-29639-03 and AAT-2-31605-02) and U.S.DOE (Contract No. DE-FC36-00GO10600).

REFERENCES

[1] R.O. Bell and J.P. Kalejs, "Growth of silicon sheets forphotovoltaic applications", *J. Mater. Res.* **13**, 1988, pp.2732-2739.

[2] S. Ostapenko, I. Tarasov, J.P. Kalejs, C. Haessler, and E.-U. Reisner, "Defect monitoring using scanning photoluminescence spectroscopy in multicrystalline silicon wafers", *Semicond. Sci. Technol.* **15**, 2000, pp.840-848.

[3] V. Alex, S. Finkbeiner, and J. Weber, "Temperature dependence of the indirect energy gap in crystalline silicon", *J. Appl. Phys.* **79**, 1996, pp.6943-6946.

[4] S. Ostapenko and M. Romero, "Defect mapping in full-size multi-crystalline Si wafers", *Eur. Phys. J. Appl. Phys.* **27**, 2004, pp.55-58.

[5] I. Tarasov et al., "Defect diagnostics using scanning photoluminescence in multicrystalline silicon", *Physica B* **273-274**, 1999, pp.549-552.

[6] D. Macdonald and A. Cuevas, "Trapping of minority carriers in multicrystalline silicon", *Appl. Phys. Lett.* **74**, 1999, pp.1710-1712.

[7] A. Ebong, P. Doshi, S. Narasimha, A. Rohatgi, J. Wang, and M.A. El-Sayed, "The effect of low and high temperature anneals on the hydrogen content and passivation of Si surface coated with SiO_2 and SiN films", *J. Electrochem. Soc.* **146**, 1999, pp1921-1924.

[8] V. Yelundur, A. Rohatgi, A. Ebong, A.M. Gabor, J. Hanoka, and W.L. Wallace, "Al-enhanced PECVD SiN_x induced hydrogen passivation in string ribbon silicon", *J. Electron. Mater.* **30**, 2001, pp.526-531.

[9] F. Duerinckx and J. Szlufcik, "Defect passivation of industrial multicrystalline solar cells based on PECVD silicon nitride", *Sol. Energy Mater. Sol. Cells* **72**, 2002, pp.231-246.

[10] W.A. Lanford and M.J. Rand, "The hydrogen content of plasma-deposited silicon nitride", *J. Appl. Phys.* **49**, 1978, pp.2473-2477.

.